Particle Accelerators, 1995, Vol. 50, pp. 83–104
Reprints available directly from the publisher
Photocopying permitted by license only

SINGLE-BEAM COLLECTIVE EFFECTS IN THE LHC

FRANCESCO RUGGIERO

SL Divison, CERN, CH-1211 GENEVA 23, Switzerland

(Received 20 February 1995; in final form 20 February 1995)

Single-beam collective effects can limit the current and therefore the performance of the Large Hadron Collider (LHC), unless the impedance of the different vacuum chamber discontinuities seen by the beam is kept below certain limits. Together with parasitic loss considerations, this has an impact on the design of several machine components, such as monitors, kickers, bellows, warm sections, experimental beam pipes, rf-cavities, feedback systems and especially on the thermal beam screen, with its millions of pumping slots. After reviewing the LHC impedance budget in view of the most recent design options, we compute rise times and thresholds for different instabilities, as well as coherent and incoherent tune shifts and parasitic losses.

KEY WORDS: Collective effects, impedances, instabilities

1 INTRODUCTION

Single-beam collective effects include incoherent phenomena, concerning the behaviour of a single particle in the electromagnetic field produced by all the others, and coherent interactions of the beam with its surroundings, usually described in terms of coupling impedances. The second group can be further subdivided into single-bunch effects, associated with the broad-band impedance of low-Q structures, and multi-bunch effects, dominated by the narrow-band impedance of high-Q resonators. Landau damping of coherent beam oscillation modes, that takes place providing their tune shifts remain within the incoherent tune spread, can be considered as a bridge between incoherent and coherent phenomena.

The main examples of incoherent effects are synchrotron radiation losses, direct space charge and Laslett tune shifts due to image currents, as well as intra-beam scattering (that we shall not discuss here). As we will see, the magnetic Laslett tune shift at injection in the LHC is of the order of 10^{-2}: this large tune shift can be compensated by adjusting the tuning quadrupoles, but sets rather stringent requirements on the equalization of the bunch populations.

Coherent effects include parasitic losses, associated with the real part of the longitudinal coupling impedance Z_{L}, and complex tune shifts of the beam oscillation modes. For Gaussian bunches, with r.m.s. bunch length $\sigma_{\mathrm{s}} = c\sigma_\tau$, the power dissipated by the wall currents in an impedance with a resistive component $\mathrm{Re}[Z_{\mathrm{L}}(\omega)]$ is

$$P = 2k_b I_b^2 \sum_{p=0}^{\infty} \mathrm{Re}\,[Z_L(p\omega_o)] \exp\left[-(p\omega_o\sigma_\tau)^2\right],$$

where k_b is the number of bunches, I_b the bunch current and ω_o the angular revolution frequency around the ring. The quadratic dependence on the bunch current is to be noted.

For a given beam intensity, the coherent oscillation modes are self-consistent solutions of the linearized Vlasov equation. They satisfy an integral equation that can be transformed into an infinite-dimensional eigenvalue problem: the eigenvectors are connected with the power spectrum of the corresponding coherent modes and the eigenvalues are the associated complex tune shifts. Note that the exact eigenvectors, as well as the eigenvalues, depend both on the coupling impedance and on the longitudinal distribution of the bunches. The latter is also a function of the current, owing to the potential well distortion.

In the limit of weak beam intensity, each mode is characterized by a number n, defining its azimuthal dependence in the longitudinal phase space. For longitudinal modes ($n = \pm 1, \pm 2, \ldots$) the unperturbed tunes are $Q_L^{(n)} = nQ_s$, while for transverse head-tail modes ($n = 0, \pm 1, \pm 2, \ldots$) the unperturbed tunes are $Q_T^{(n)} = Q_\beta + nQ_s$, where Q_s denotes the synchrotron tune and Q_β the betatron tune. When observed at a fixed location around the ring, the signal corresponding to each oscillation mode consists of discrete spectral lines at frequencies

$$\omega_p = \begin{cases} \omega_o\,(pk_b + m + nQ_s) & \text{for longitudinal modes,} \\ \omega_o\,(pk_b + m + nQ_s + Q_\beta) & \text{for transverse modes.} \end{cases}$$

Here m denotes the coupled-bunch mode number ($0 \le m \le k_b - 1$).

To specify uniquely a given coherent mode, one should also assign its radial dependence in the longitudinal phase space. For vanishing beam intensities, modes with the same azimuthal number n and different radial dependence have the same tune $Q^{(n)}$, but this degeneracy is progressively removed for increasing beam currents. However, if the tune shifts remain much smaller than Q_s, different radial modes will couple only when they belong to the same azimuthal family n: such regime of weak beam intensity is governed by the so-called Sacherer integral equation. A further simplification is obtained by neglecting the possible coupling between radial modes with the same n (e.g., when the problem can be exactly or approximately diagonalized analytically) and expressing the complex tune shift of the most prominent radial mode in terms of its *effective impedance*,[1] measuring the degree to which the impedance overlaps the mode spectrum. Then the complex tune shift for longitudinal modes is approximately given by

$$\Delta Q_L^{(m,n)} = -j \frac{|n|}{|n|+1} \frac{Q_s I_b}{3h_{rf}V_{rf}} \left(\frac{2\pi R}{L}\right)^3 \left(\frac{Z_L}{n}\right)_{\mathrm{eff}}^{(m,n)}, \tag{1}$$

where h_{rf} and V_{rf} are the harmonic number and peak rf-voltage, respectively, R is the average machine radius, $L = 4\sigma_s$ the full bunch length and the effective longitudinal impedance is defined by

$$\left(\frac{Z_L}{n}\right)_{\text{eff}}^{(m,n)} = \frac{\sum_{p=-\infty}^{\infty} \frac{Z_L(\omega_p)}{\omega_p/\omega_0} h_{|n|}(\omega_p)}{\sum_{p=-\infty}^{\infty} h_{|n|}(\omega_p)}.$$

Here $h_n(\omega)$ denotes the mode power spectrum and, for Gaussian bunches, it is

$$h_n(\omega) = \frac{(\omega\sigma_\tau)^{2n}}{\Gamma(n+1/2)} \exp\left[-(\omega\sigma_\tau)^2\right].$$

Similarly, the complex tune shift for transverse modes is approximately given by

$$\Delta Q_T^{(m,n)} = \frac{j}{|n|+1} \frac{I_b R}{2(E/e)L} \beta_{\text{av}} (Z_T)_{\text{eff}}^{(m,n)}, \tag{2}$$

where β_{av} is the average betatron function, E/e the beam energy in volts and the effective transverse impedance is defined by

$$(Z_T)_{\text{eff}}^{(m,n)} = \frac{\sum_{p=-\infty}^{\infty} Z_T(\omega_p) h_{|n|}(\omega_p - \omega_\xi)}{\sum_{p=-\infty}^{\infty} h_{|n|}(\omega_p - \omega_\xi)}.$$

In the following, we shall not consider the chromatic shift $\omega_\xi = Q'\omega_0/\eta$ associated with the chromaticity Q' and the slippage factor η.

From Eqs. (1) and (2), we see that the imaginary part of the effective impedance is responsible for (real) coherent tune shifts and can lead to collective instabilities owing to mode coupling or to loss of Landau damping, while the real part of the effective impedance is related to the instability rise time. In the following, we show that the bunch population in the LHC is limited to about 2.4×10^{11} protons, owing to suppression of Landau damping for longitudinal high-order modes at 7 TeV. The transverse resistive wall instability has a rise time longer than 100 revolution periods and can thus be cured by feedback. However the LHC impedance budget is not yet complete and requires more detailed calculations.

2 SPACE CHARGE EFFECTS

The space charge of the beam gives rise to a detuning of the incoherent particle oscillations and affects the collective behaviour of the beam oscillation modes. We first discuss the detuning caused by the direct space charge effect, which for the LHC is significant only at injection, and then the Laslett tune shifts associated with image currents induced on the beam pipe and on the ferromagnetic magnet poles. Finally we consider the space charge impedance, which dominates the transverse impedance budget at injection energy.

2.1 *Direct space charge tune shift*

For a *round* beam, the tune shift of particles with *small* betatron amplitude due to direct space charge is

$$\Delta Q_{\mathrm{dsc}} = -\frac{N_{\mathrm{b}} r_{\mathrm{p}}}{4\pi B \beta \gamma^2 \epsilon_{\mathrm{N}}} = \begin{cases} -1.2 \times 10^{-3} & \text{at 450 GeV,} \\ -1.1 \times 10^{-5} & \text{at 7 TeV.} \end{cases} \tag{3}$$

Here $N_{\mathrm{b}} = 10^{11}$ is the number of particles per bunch, $r_{\mathrm{p}} = 1.5347 \times 10^{-18}$ m the classical proton radius, $\gamma = (1 - \beta^2)^{-1/2}$ the Lorentz factor, B the bunching factor and $\epsilon_{\mathrm{N}} = \epsilon\beta\gamma = 3.75 \times 10^{-6}$ m rad is the normalized beam emittance. In Eq. (3) we have used

$$\gamma = \begin{cases} 479.6 & \text{at 450 GeV,} \\ 7460.5 & \text{at 7 TeV,} \end{cases} \qquad B = \frac{\sqrt{2\pi}\sigma_{\mathrm{s}}}{2\pi R} = \begin{cases} 1.22 \times 10^{-5} & \text{at 450 GeV,} \\ 7.05 \times 10^{-6} & \text{at 7 TeV,} \end{cases}$$

with $R = 4242.89$ denoting the average machine radius and σ_{s} the r.m.s. bunch length, equal to 13 cm at injection and to 7.5 cm at 7 TeV.

The direct space charge tune shift is smaller for particles with larger betatron amplitudes and the resulting incoherent tune spread gives rise to Landau damping of transverse beam oscillations (with the exception of rigid dipole oscillations).

2.2 *Laslett tune shift*

Owing to image currents induced on the beam pipe and on the ferromagnetic magnet poles, *all particles* suffer another incoherent detuning having opposite sign in the two betatron planes. The vertical Laslett tune shift is given by

$$\Delta Q_{\mathrm{Laslett}} = -\frac{N_{\mathrm{b}} k_{\mathrm{b}} r_{\mathrm{p}} \beta_{\mathrm{av}}}{\pi\gamma} \left(\frac{\varepsilon_1}{h^2} + \frac{\varepsilon_2}{g^2} \right) \simeq \begin{cases} -1.7 \times 10^{-2} & \text{at 450 GeV,} \\ -1.1 \times 10^{-3} & \text{at 7 TeV,} \end{cases} \tag{4}$$

where $k_{\mathrm{b}} = 2835$ is the number of bunches and $\beta_{\mathrm{av}} = 85$ m the average betatron function. The electric and magnetic Laslett coefficients ε_1 and ε_2 depend on the geometry of the beam pipe (with half-height h) and of the ferromagnetic magnet poles (with distance $2g \simeq 5$ cm). For a beam pipe of circular or square cross section we have $\varepsilon_1 = 0$, while assuming plane magnet poles yields $\varepsilon_2 = 0.41$; these values have been used to compute the Laslett tune shift in Eq. (4), since a more realistic estimate of the magnetic coefficient ε_2 for the circular geometry of the cold bore is still missing. At injection energy the tune shift is large, but can be compensated by adjusting the tuning quadrupoles. However this sets rather stringent requirements on the equalization of the bunch populations N_{b}.

For a beam offset of 10% of the pipe 'radius', the electric coefficient would become $\varepsilon_1 \leq 0.01$, depending on the direction of the closed orbit deviation relative to the diagonals of the square beam screen (see Figure 1a). Indeed the horizontal and vertical Laslett coefficients form a non diagonal second-rank *tensor*,[2] with 'normal modes' oriented at 45° from these diagonals. The consequences of this effect on betatron coupling should be further investigated.

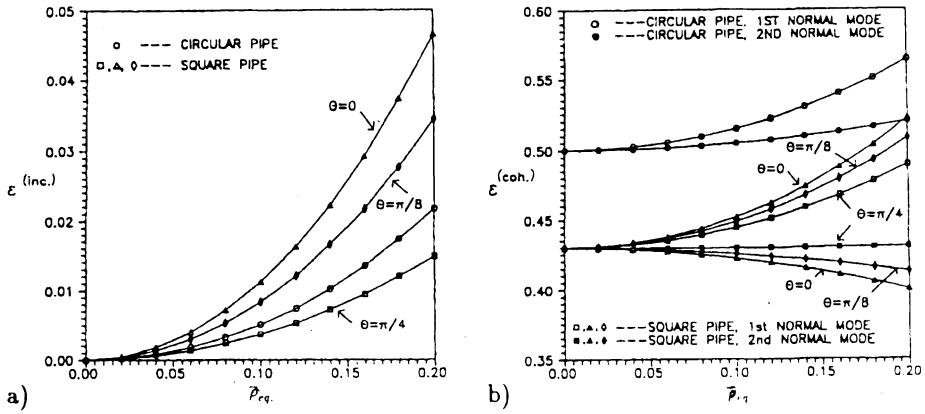

FIGURE 1: Principal values of the incoherent (a) and coherent (b) electric Laslett tensors versus the beam offset from the center of a square pipe, for different angular directions θ, and for the inscribed circular pipe:[2] the beam offset $\bar{\rho}_{\rm eq}$ is scaled by the radius of the inscribed circle. For a beam offset in a given angular direction ($\theta=\pi/4$ corresponding to the diagonal of the square), there are two normal modes of oscillation and, in case of a circular pipe, one of them is in the radial direction. The two principal values of the incoherent Laslett tensor have opposite sign, but only the positive one is plotted in figure (a).

It is worth mentioning that, in the derivation of the space charge tune shifts,[3] one usually starts from the Lorentz force $F_{\rm y} = e(E_{\rm y}+\beta B_{\rm x})$ and applies the proper boundary conditions for a round beam of radius $a = \sqrt{2\epsilon\beta_{\rm av}}$ with uniform charge distribution in the transverse plane. The vertical tune shift is then given by an expression of the type

$$\Delta Q \propto \underbrace{-\frac{1}{B'\beta^2}\left(1+\varepsilon_1\frac{2a^2}{h^2}\right)}_{\text{electric}} + \underbrace{\left(1-\varepsilon_2\frac{2a^2}{g^2}\right)}_{\text{dc magnetic}} + \underbrace{\left(\frac{1}{B'}-1\right)\left(1+\varepsilon_1\frac{2a^2}{h^2}\right)}_{\text{ac magnetic}},$$

where the first term corresponds to the effect of the electric field, while the magnetic contribution is split into a 'dc' and an 'ac' part. The proportionality constant is $(\lambda_{\rm av} R r_{\rm p}\beta_{\rm av})/(a^2\gamma)$, where $\lambda_{\rm av}$ is the average beam density, and B' denotes the ratio of the average to the peak density:

$$\lambda_{\rm av} = \frac{N_{\rm b}k_{\rm b}}{2\pi R}, \qquad B' = \frac{\lambda_{\rm av}}{\lambda_{\rm max}} = \frac{N_{\rm b}k_{\rm b}/2\pi R}{N_{\rm b}/\sqrt{2\pi}\sigma_{\rm s}} = k_{\rm b}\frac{\sqrt{2\pi}\sigma_{\rm s}}{2\pi R} = k_{\rm b}B.$$

Finally one assumes no leakage of the 'ac' magnetic contribution and thus obtains

$$\Delta Q = \frac{N_{\rm b}k_{\rm b}r_{\rm p}\beta_{\rm av}}{2\pi a^2\gamma}\left[\frac{1}{B'}\left(1-\frac{1}{\beta^2}\right)\left(1+\varepsilon_1\frac{2a^2}{h^2}\right)-\left(\varepsilon_1\frac{2a^2}{h^2}+\varepsilon_2\frac{2a^2}{g^2}\right)\right]$$

$$= \frac{N_{\rm b}k_{\rm b}r_{\rm p}\beta_{\rm av}}{2\pi a^2\gamma}\left[-\frac{1}{k_{\rm b}B}\frac{1}{\beta^2\gamma^2}\left(1+\varepsilon_1\frac{2a^2}{h^2}\right)-2a^2\left(\frac{\varepsilon_1}{h^2}+\frac{\varepsilon_2}{g^2}\right)\right].$$

In the last step there is a relativistic cancellation of electric and magnetic terms, leading to the separation of the direct space charge tune shift ΔQ_{dsc} of Eq. (3), inversely proportional to $\beta\gamma^2\epsilon_{\mathrm{N}}$ and obtained neglecting the small correction of order a^2/h^2, from the Laslett tune shift of Eq. (4). However, during the filling of the machine, there can be some leakage of the ac magnetic field at very low frequencies (comparable to the revolution frequency of 11 kHz) and consequently a transient bunch-to-bunch tune variation $\Delta Q \sim \gamma^2 \Delta Q_{\mathrm{dsc}} \varepsilon_1 2a^2/h^2 \sim \varepsilon_1$. This possibility should be studied more carefully, since such a detuning cannot be compensated by adjusting the quadrupoles.

2.3 *Space charge impedance*

In addition to incoherent tune shifts, space charge forces also affect the collective behaviour of the beam. They can be characterized by purely imaginary coupling impedances[4] that, contrary to the ordinary case, depend both on the vacuum chamber geometry and on beam properties, such as the Lorentz factor γ and the r.m.s. beam radius $a = \sqrt{\epsilon\beta_{\mathrm{av}}}$ (note the difference by a factor $\sqrt{2}$ compared to the a of the previous subsection).

For a smooth vacuum pipe of radius $b = 17.4$ mm (i.e. inscribed in the square cross section of the LHC liner), the coupling impedances are:

$$Z_{\mathrm{L}}(\omega) = -j\,\frac{\omega R}{2c}\,\frac{Z_{\mathrm{o}}}{\gamma^2}\left[1 + 2\ln\left(\frac{b}{a}\right)\right],$$

$$Z_{\mathrm{T}}(\omega) = -j\,\frac{Z_{\mathrm{o}} R}{\gamma^2}\left(\frac{1}{2a^2} - \frac{1}{b^2}\right),$$

where $Z_{\mathrm{o}} = 376.73\ \Omega$ is the free space impedance and c the speed of light. At injection energy, when $a = 0.815$ mm, we have

$$\frac{Z_{\mathrm{L}}}{n} = -j\,5.8\ \mathrm{m}\Omega, \qquad \beta_{\mathrm{av}} Z_{\mathrm{T}} = -j\,442.4\ \mathrm{M}\Omega$$

and the coherent tune shifts of the lowest longitudinal and transverse modes, computed according to Eqs. (1) and (2) for a nominal bunch population $N_{\mathrm{b}} = 10^{11}$ particles, are given in Table 1. At 7 TeV, when $a = 0.207$ mm, we have

$$\frac{Z_{\mathrm{L}}}{n} = -j\,3.3 \times 10^{-5}\ \Omega, \qquad \beta_{\mathrm{av}} Z_{\mathrm{T}} = -j\,28.6\ \mathrm{M}\Omega$$

and the corresponding coherent tune shifts can be neglected.

TABLE 1: Coherent space charge tune shifts at injection.

Longitudinal tune shifts	Transverse tune shifts
	$\Delta Q_{\mathrm{T}}^{(0)} = 7.49\times10^{-4}$
$\Delta Q_{\mathrm{L}}^{(1)} = -4.64\times10^{-7}$	$\Delta Q_{\mathrm{T}}^{(1)} = 3.75\times10^{-4}$
$\Delta Q_{\mathrm{L}}^{(2)} = -6.18\times10^{-7}$	$\Delta Q_{\mathrm{T}}^{(2)} = 2.50\times10^{-4}$
$\Delta Q_{\mathrm{L}}^{(3)} = -6.96\times10^{-7}$	$\Delta Q_{\mathrm{T}}^{(3)} = 1.87\times10^{-4}$

The transverse space charge impedance is a tensor with properties similar to those of the Laslett coefficients:[2] as shown in Figure 1b, the principal values of the Laslett tensor for coherent transverse dipole oscillations in a beam screen with square cross section are slightly smaller than the values corresponding to the inscribed circular pipe. Therefore, in establishing the LHC impedance budget, we shall use the previous simpler results valid for the pessimistic choice of the inscribed circular pipe.

3 BROAD-BAND RESONATORS

Besides coherent space charge effects and pumping slots in the beam screen, the main sources of broad-band impedance in the LHC are bellows and monitor tanks. The longitudinal and transverse coupling impedances of these elements will be parameterized by the superposition of a few resonant contributions with low quality factors Q_L and Q_T:

$$Z_L(\omega) = \frac{R_L}{1 - jQ_L\left(\frac{\omega_{rL}}{\omega} - \frac{\omega}{\omega_{rL}}\right)}, \tag{5}$$

$$Z_T(\omega) = \frac{R_T}{1 - jQ_T\left(\frac{\omega_{rT}}{\omega} - \frac{\omega}{\omega_{rT}}\right)}\frac{\omega_{rT}}{\omega}, \tag{6}$$

where ω_{rL} and ω_{rT} are the resonant frequencies, while R_L and R_T are the longitudinal and transverse shunt impedances.

A final design of the LHC bellows shielding is not yet available, therefore we consider the geometry of the SSC bellows[5] and approximate the longitudinal impedance of a single bellows package by two broad-band resonators with shunt impedances 20 Ω and 30 Ω, resonant frequencies 6.2 GHz and 16 GHz and quality factors 6 and 1, respectively. The transverse impedance is approximated by a resonator with shunt impedance 1.9 kΩ/m, resonant frequency 2.8 GHz and quality factor 3.5. The low-frequency impedances amount to $Z_L/n = j\,0.08$ Ω and $Z_T = j\,1.6$ MΩ/m. This is for a total number of 3000 bellows, comparable to the number of bellows in LEP, and the broad-band resonator parameters are summarized in Table 2. The total transverse impedance measured for the LEP shielded bellows is $Z_T = j\,0.16$ MΩ/m. Since the vertical aperture of the LEP vacuum chamber is $b = 3.5$ cm and Z_T scales with the inverse of the second to third power of the pipe radius, this leads to a value in agreement with our estimate for the LHC, under the pessimistic assumption of a reduced pipe radius $b = 1.5$ cm (equal to the SSC value).

The influence of the shallow cavities which house the 500 strip-line monitors has been approximated[6,7] by a broad-band resonator with a quality factor $Q = 1$, a resonant frequency of 6 GHz and a low-frequency inductance $Z_L/n = j\,0.04$ Ω. The resistive part of the impedance rises only above the pipe cut-off frequency and, for a single monitor tank, it reaches an average value of 20 Ω at about twice this frequency. Its contribution to the cryogenic heat load is therefore negligible,[8] since there is practically no overlap with the bunch power spectrum. The transverse impedance is obtained from the longitudinal one

TABLE 2: Global parameters for the broad-band resonators.

Longitudinal	$\omega_{rL}/2\pi$	Q_L	R_L
shielded bellows	6.2 GHz	6	60 kΩ
shielded bellows	16 GHz	1	90 kΩ
monitor tanks	6 GHz	1	21.3 kΩ
Transverse	$\omega_{rT}/2\pi$	Q_T	$\beta_{av} \times R_T$
shielded bellows	2.8 GHz	3.5	85×5.7 MΩ
monitor tanks	6 GHz	1	172.8×1.17 MΩ

by using the same relation as in the case of the resistive wall, although for any structure other than a smooth pipe this relation is only approximate

$$Z_T = \frac{2R}{b_{eff}^2} \frac{Z_L}{n}, \tag{7}$$

assuming an effective beam pipe radius $b_{eff} = 1.7$ cm. The corresponding broad-band resonator parameters are reported in Table 2.

Since all the broad-band resonators have resonant frequencies of several GHz and the power spectrum of the lowest modes is typically below 1 GHz, their effective impedance does not depend very much on the azimuthal mode number. The total effective impedances associated with the broad-band resonators for the lowest longitudinal and transverse modes at injection are

$$\left(\frac{Z_L}{n}\right)_{eff} = j\,81.5\ \text{m}\Omega, \qquad \beta_{av}\,(Z_T)_{eff} = j\,139.5\ \text{M}\Omega \qquad \text{for shielded bellows,}$$

$$\left(\frac{Z_L}{n}\right)_{eff} = j\,40.0\ \text{m}\Omega, \qquad \beta_{av}\,(Z_T)_{eff} = j\,203.0\ \text{M}\Omega \qquad \text{for monitor tanks,}$$

and the coherent tune shifts of a few low-order modes, computed according to Eqs. (1), (2), (5) and (6) for a nominal bunch population $N_b = 10^{11}$ particles, are given in Table 3.

TABLE 3: Coherent tune shifts at injection due to the broad-band resonators.

Longitudinal tune shifts	Transverse tune shifts
	$\Delta Q_T^{(0)} = -5.80\times10^{-4}$
$\Delta Q_L^{(1)} = 9.66\times10^{-6}$	$\Delta Q_T^{(1)} = -2.92\times10^{-4}$
$\Delta Q_L^{(2)} = 1.29\times10^{-5}$	$\Delta Q_T^{(2)} = -1.96\times10^{-4}$
$\Delta Q_L^{(3)} = 1.45\times10^{-5}$	$\Delta Q_T^{(3)} = -1.48\times10^{-4}$

TABLE 4: Coherent tune shifts at injection due to strip-line monitors.

Longitudinal tune shifts	Transverse tune shifts
	$\Delta Q_{\mathrm{T}}^{(0)} = -7.56\times10^{-4}$
$\Delta Q_{\mathrm{L}}^{(1)} = 1.28\times10^{-7}$	$\Delta Q_{\mathrm{T}}^{(1)} = -4.80\times10^{-6}$
$\Delta Q_{\mathrm{L}}^{(2)} = -4.34\times10^{-7}$	$\Delta Q_{\mathrm{T}}^{(2)} = 8.16\times10^{-6}$
$\Delta Q_{\mathrm{L}}^{(3)} = 2.80\times10^{-7}$	$\Delta Q_{\mathrm{T}}^{(3)} = -3.51\times10^{-6}$

4 LOW FREQUENCY IMPEDANCE

Strip-line monitors and abort kickers are the main sources of low-frequency impedance. They contribute essentially to the coherent tune shift of the lowest head-tail mode.

The coupling impedances of the beam position monitors, consisting of *two* strip lines with length $\ell = 30$ cm, each subtending an azimuthal angle $\phi = 110^\circ \times 2\pi/360$ rad and having a characteristic impedance $Z_{\mathrm{s}} = 50\ \Omega$, are

$$Z_{\mathrm{L}}(\omega) = 2N_{\mathrm{m}}Z_{\mathrm{s}}\left(\frac{\phi}{2\pi}\right)^2 \sin\left(\frac{\omega\ell}{c}\right)\left[\sin\left(\frac{\omega\ell}{c}\right) + j\cos\left(\frac{\omega\ell}{c}\right)\right],$$

$$Z_{\mathrm{T}}(\omega) = \frac{1}{2}\frac{c}{b^2}\left(\frac{4}{\phi}\right)^2 \sin^2\left(\frac{\phi}{2}\right)\frac{Z_{\mathrm{L}}(\omega)}{\omega},$$

where $N_{\mathrm{m}} = 500$ is the total number of monitors and we have assumed that each strip-line plate has a radial distance $b = 17.4$ mm from the beam axis. Monitors are provided close to each quadrupole to measure the horizontal *or* vertical beam position and the factor $1/2$ appearing in the transverse impedance Z_{T} accounts for the fact that only half of the monitors contribute in a given plane; the betatron function to be used in Eq. (2) for the transverse tune shifts is however $\beta_{\max} = 172.8$ m, i.e. the maximum beta in the regular arc. If the monitors were equipped with four strip lines, to measure the horizontal and vertical beam position at the same time, the longitudinal impedance would be multiplied by a factor two but the transverse tune shifts would remain almost the same, since half of the monitors would be at the minimum beta $\beta_{\min} = 30.3$ m.

The tune shifts at injection for a nominal bunch population $N_{\mathrm{b}} = 10^{11}$ are shown in Table 4: as can be seen, the only significant contribution is that to the transverse dipole tune shift $\Delta Q_{\mathrm{T}}^{(0)}$. The effective impedances, defined here as the overlap integrals with the bunch power spectrum $h_{\mathrm{o}}(\omega)$, are

$$\left(\frac{Z_{\mathrm{L}}}{n}\right)_{\mathrm{eff}} = j\ 127\ \mathrm{m}\Omega, \qquad \beta_{\mathrm{av}}\,(Z_{\mathrm{T}})_{\mathrm{eff}} = j\ 446.6\ \mathrm{M}\Omega \qquad \text{at injection},$$

$$\left(\frac{Z_{\mathrm{L}}}{n}\right)_{\mathrm{eff}} = j\ 73\ \mathrm{m}\Omega, \qquad \beta_{\mathrm{av}}\,(Z_{\mathrm{T}})_{\mathrm{eff}} = j\ 257.9\ \mathrm{M}\Omega \qquad \text{at 7 TeV}.$$

The LHC abort kicker magnets are located at a very high-beta region, with $\beta_{av} = 600$ m, and extend over a total length $L = 14 \times 1.26$ m. They are equipped with a ceramic vacuum chamber of thickness $\Delta = 4.5$ mm, width $w = 40$ mm and height $h = 28$ mm. The inside of the chamber has a titanium coating of thickness $d = 1$ μm to reduce the high-frequency impedance seen by the beam and to conduct away the static charge.[9] Moreover, two copper plates between the H-shaped ferrites on the outside of the ceramic chamber reduce the low-frequency impedance, by carrying most of the beam image currents. Assuming an electric permeability $\epsilon = 10$ for the ceramic and considering the pessimistic case of a circular pipe with radius $b = h/2 = 14$ mm, the coupling impedances at frequencies well below $\omega/2\pi \sim c/(2\pi\sqrt{\epsilon}b) = 1$ GHz can be written[10]

$$Z_L(\omega) = Z_o \frac{\omega L}{4\pi c} \frac{s(\omega) + j\zeta}{s(\omega)^2 + \zeta^2},$$

$$Z_T(\omega) = \frac{2c}{b^2} \frac{Z_L(\omega)}{\omega},$$

where $\sqrt{s(\omega)}$ is the ratio between the geometric mean of the pipe radius and the coating thickness, on one side, and the skin-depth $\delta_{Ti}(\omega)$ in the titanium, having resistivity $\rho_{Ti} = 7 \times 10^{-7}$ Ωm,

$$s(\omega) = \frac{bd}{\delta_{Ti}^2(\omega)}, \qquad \delta_{Ti}(\omega) = \sqrt{\frac{2\rho_{Ti}}{\mu_o \omega}}, \qquad \zeta = \frac{(b+\Delta)^2}{(b+\Delta)^2 - b^2} = 2.34.$$

The corresponding low-frequency values of Z_L/n and $\beta_{av} Z_T$ are

$$\frac{Z_L}{n} = j\,53\ \text{m}\Omega, \qquad \beta_{av} Z_T = j\,1384\ \text{M}\Omega, \qquad \text{for } \omega \to 0.$$

As shown in Figure 2, the real part of Z_T has a peak around the bunch frequency $k_b \omega_o/2\pi \sim 30$ MHz, corresponding to $\beta_{av}\text{Re}(Z_T^{\max}) = 692$ MΩ. The tune shifts of the transverse coherent modes have therefore an imaginary part depending on the coupled-bunch mode number m; its maximum value at injection is $\max\left[\text{Im}\left(\Delta Q_T^{(m,n)}\right)\right] = \text{Im}\left(\Delta Q_T^{(2045,0)}\right) \simeq 2 \times 10^{-6}$, corresponding to a very weak coupled-bunch instability of the transverse dipole mode with a rise time of about 7 sec, easily cured by feed-back. The real parts of the longitudinal and transverse tune shifts depend very little on m. They are reported in Table 5 for the lowest coherent modes, assuming $N_b = 10^{11}$: the only significant contribution is that to the transverse dipole tune shift $\Delta Q_T^{(o)}$. The effective impedances, defined again as the overlap integrals with the bunch power spectrum $h_o(\omega)$, are

$$\left(\frac{Z_L}{n}\right)_{\text{eff}} = j\,7\ \text{m}\Omega, \qquad \beta_{av}\,(Z_T)_{\text{eff}} = j\,181.2\ \text{M}\Omega \qquad \text{at injection},$$

$$\left(\frac{Z_L}{n}\right)_{\text{eff}} = j\,4\ \text{m}\Omega, \qquad \beta_{av}\,(Z_T)_{\text{eff}} = j\,108.5\ \text{M}\Omega \qquad \text{at 7 TeV}.$$

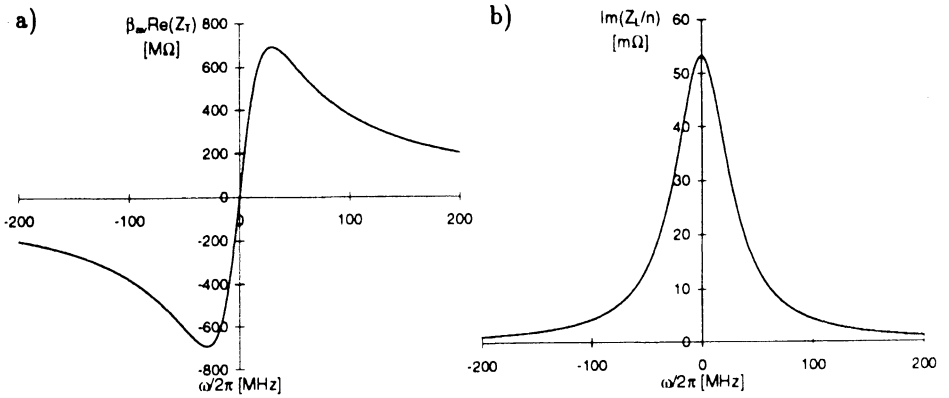

FIGURE 2: Average beta times the real part of the transverse impedance Z_T in MΩ (a) and imaginary part of the longitudinal impedance Z_L/n in mΩ (b) versus the frequency $\omega/2\pi$ in MHz, for the LHC abort kickers.

It is worth mentioning that, owing to the shielding by eddy currents, the maximum surface resistance $R_\square^{\max}$ compatible with the required kicker rise time $\tau_k = 3\ \mu$s would be

$$R_\square^{\max} = \frac{\mu_o w}{\pi k \tau_k} = 53\ \text{m}\Omega,$$

where we have assumed a safety factor $k = 0.1$ between the rise time due to shielding and the kicker rise time τ_k, corresponding to more than 99% of the maximum field after a time equal to τ_k for a δ-like variation of the external magnetic field. Therefore, the associated maximum thickness of the titanium layer could be

$$d^{\max} = \frac{\rho_{Ti}}{R_\square^{\max}} = 13.1\ \mu\text{m}.$$

At the moment, however, there is no stringent argument in favour of a thicker titanium coating of the ceramic chamber, whose technical realization would also be rather difficult.

TABLE 5: Real parts of the coherent tune shifts at injection due to abort kickers.

Longitudinal tune shifts	Transverse tune shifts
	$\Delta Q_T^{(0)} = -3.08\times10^{-4}$
$\Delta Q_L^{(1)} = 4.80\times10^{-8}$	$\Delta Q_T^{(1)} = -1.33\times10^{-5}$
$\Delta Q_L^{(2)} = 2.43\times10^{-8}$	$\Delta Q_T^{(2)} = -3.36\times10^{-6}$
$\Delta Q_L^{(3)} = 1.65\times10^{-8}$	$\Delta Q_T^{(3)} = -1.52\times10^{-6}$

5 BEAM SCREEN AND PUMPING SLOTS

As shown in Figure 1 of Reference 11, the LHC beam screen has a square cross section with rounded corners; the radius of the inscribed circle is $b = 17.4$ mm and the radius of curvature of the rounded corners is almost exactly equal to $b/2$. The stainless steel screen has a thickness of 1 mm and its inside is coated with a copper layer of thickness $t = 50$ μm and residual resistance ratio RRR $\sim$ 100. Since the screen is at a temperature $T \sim 20°$ K, the corresponding copper resistivity is $\rho_{Cu} = 1.8 \times 10^{-10}$ Ωm at injection and $\rho_{Cu} = 5.5 \times 10^{-10}$ Ωm at top energy, respectively, taking due account of the magnetoresistance effect in a magnetic field $B = 0.56$ Tesla at injection and $B = 8.65$ Tesla at 7 TeV. The stainless steel resistivity is $\rho_{SS} = 5 \times 10^{-7}$ Ωm.

As sketched in Figure 1 of Reference 12, in the beam screen there are 500 rectangular slots per meter. Each slot has a length $\ell = 8$ mm and a width $w = 1.5$ mm, with rounded edges; the corresponding fractional surface of beam screen covered by slots is 4.3%, which is sufficient for vacuum pumping considerations. The slots are staggered along two rows located at a distance of $b/2$ from the middle of each screen side, i.e., just where the rounded corners touch the sides of the square, and their arrangement is such that each cross section of the screen contains four slots. The induced image currents at the slot positions have been numerically computed to be smaller by a factor 0.79, compared to the case of a round screen with radius b. This gives a geometric reduction factor $f_{geom} = 0.63 = (0.79)^2$ for the longitudinal slot impedance and we assume the same geometric factor also for the transverse impedance, although the analytic result for a perfectly square screen cross section is about 15% lower. A further reduction factor $f_{th} = 0.6$ comes from the finite thickness of the beam screen. Finally, the aspect ratio $\ell/w = 5.\overline{3}$ of the LHC slots corresponds[13] to a relative polarizability $\alpha_{rel} = 1.5$ compared to the case of round holes with radius $r_h = w/2$. In conclusion, the total coupling impedances of the pumping slots can be obtained by computing the impedances of $N_h = 500 \times 2\pi R/\text{m} = 13.3$ millions of round holes, in a thin round screen inscribed in the square LHC liner, and then multiplying the result by a global reduction factor F

$$F = f_{geom} f_{th} \alpha_{rel} = 0.56.$$

This yields

$$\frac{Z_L}{n} = j N_h \frac{Z_o}{R} \frac{\frac{2}{3} r_h^3}{4\pi^2 b^2} F = j\, 15.6\ \text{m}\Omega,$$

$$Z_T = \frac{2R}{b^2} \frac{Z_L}{n} = j\, 0.44\ \text{M}\Omega/\text{m}.$$

The latter corresponds to a weighted transverse impedance $\beta_{av} Z_T = j\, 37.1$ MΩ. The corresponding tune shifts at injection, for a nominal bunch population $N_b = 10^{11}$, are shown in Table 6.

In addition to these inductive impedances, the pumping slots may give rise to high-Q trapped modes with frequencies slightly below the screen cut-off frequency and associated with narrow-band impedances having high peak values of $Z_L/n \sim 300$ Ω:[13] according

TABLE 6: Coherent tune shifts at injection due to pumping slots.

Longitudinal tune shifts	Transverse tune shifts
	$\Delta Q_{\mathrm{T}}^{(0)} = -6.28 \times 10^{-5}$
$\Delta Q_{\mathrm{L}}^{(1)} = 1.29 \times 10^{-6}$	$\Delta Q_{\mathrm{T}}^{(1)} = -3.14 \times 10^{-5}$
$\Delta Q_{\mathrm{L}}^{(2)} = 1.72 \times 10^{-6}$	$\Delta Q_{\mathrm{T}}^{(2)} = -2.09 \times 10^{-5}$
$\Delta Q_{\mathrm{L}}^{(3)} = 1.94 \times 10^{-6}$	$\Delta Q_{\mathrm{T}}^{(3)} = -1.57 \times 10^{-5}$

to preliminary estimates,[14] the maximum acceptable value of Z_{L}/n for beam stability is around 15 Ω. Therefore, the present base-line design of the LHC beam screen includes a 10% randomization of the slot lengths, leading to a reduction of their effective quality factors and of the corresponding narrow-band impedance by a factor 20. The slot spacing should also be randomized, to damp possible higher-frequency travelling modes associated with the periodic slot pattern.

6 OTHER SOURCES OF IMPEDANCE

The LHC rf-system consists of two sets of four superconducting cavities with fundamental frequency of 400.8 MHz. At frequencies below 765 MHz, which is the cut-off frequency of the 30 cm diameter drift tubes, the impedance of these cavities has sharp resonances corresponding to the fundamental and higher cavity modes, while the low-frequency inductance is estimated to be $Z_{\mathrm{L}}/n = j\,10$ mΩ. Assuming an average beta-function $\beta_{\mathrm{av}} \simeq 100$ m at the location of the superconducting rf-cavities and using the approximate relation Eq. (7) with an effective pipe radius $b_{\mathrm{eff}} = 15$ cm, yields a very modest weighted transverse impedance $\beta_{\mathrm{av}} Z_{\mathrm{T}} \simeq 0.4$ MΩ: in the following, we make the pessimistic assumption that these low-frequency values be treated as effective impedances. Possible coupled-bunch instabilities associated with the narrow-band impedance of superconducting and septum cavities, required for longitudinal feedback, are discussed in Section 8.

Other sources of impedance are the so-called experimental chambers, having a rather small low-frequency inductance $Z_{\mathrm{L}}/n \sim j\,1.6$ mΩ,[a] recombination chambers, where two vacuum beam pipes merge into one, beam collimators, injection kickers and septa, gate valves, electrostatic transverse dampers and aperture transitions, such as warm-to-cold and square-to-round transitions. The total number of these elements and their design are still subject to significant modifications, therefore their contribution is not yet included in the impedance budget discussed in the next section.

[a] This result has been recently obtained by Y.H. Chin, using his code ABCI with a 2 mm mesh size in the radial direction. The structure, shown in Figure 11 of Reference 12, is 20 m long and has a maximum radial extent of 25 cm, with a minimum radius of 2.5 cm. Owing to the small tapering angle, a fine radial mesh is required to perform a sufficiently accurate calculation: the inductance previously obtained using an 8 mm mesh size was overestimated by a factor two. The frequencies, quality factors and shunt impedances of trapped modes in the structure have recently been computed by V.P. Yakovlev, using his code SUPERLANS.

7 IMPEDANCE BUDGET AND INSTABILITY THRESHOLDS

According to the impedance catalogue discussed in the previous sections, the total effective impedance of the LHC at injection and at top energy is summarized in Tables 7 and 8, respectively. We recall that the effective low-frequency impedances have been defined as the overlap integrals with the bunch power spectrum $h_0(\omega)$; this coincides with the conventional definition for the transverse dipole mode ($n = 0$) and gives a weighted average of the longitudinal impedance Z_L/n, although the lowest longitudinal mode corresponds to $n = 1$.

TABLE 7: LHC effective impedance (in Ω) at 450 GeV.

Injection	$\mathrm{Im}(Z_L/n)_{\mathrm{eff}}$	$\beta_{\mathrm{av}}\mathrm{Im}(Z_T)_{\mathrm{eff}}\times 10^{-6}$
Space charge	−0.0058	−442.4
Shielded bellows	0.0815	139.5
Monitor tanks	0.0400	203.0
Pumping slots	0.0156	37.1
Total broad band	0.1313	−62.8
Strip-line monitors	0.127	446.6
Abort kickers	0.007	181.2
SC cavities	0.010	0.4
Total low frequency	0.144	628.2

TABLE 8: LHC effective impedance (in Ω) at 7 TeV.

Top Energy	$\mathrm{Im}(Z_L/n)_{\mathrm{eff}}$	$\beta_{\mathrm{av}}\mathrm{Im}(Z_T)_{\mathrm{eff}}\times 10^{-6}$
Space charge	-3.3×10^{-5}	−28.6
Shielded bellows	0.0815	139.5
Monitor tanks	0.0400	203.0
Pumping slots	0.0156	37.1
Total broad band	0.1371	351.0
Strip-line monitors	0.073	257.9
Abort kickers	0.004	108.5
SC cavities	0.010	0.4
Total low frequency	0.087	366.8

7.1 *Longitudinal single-bunch effects*

The threshold bunch current I_b^{th} for the longitudinal microwave instability can be written

$$I_b^{th} \simeq \frac{3}{2} \frac{h_{rf} V_{rf}}{|(Z_L/n)_{eff}|} \left(\frac{L}{2\pi R} \right)^3 ,$$

where $L = 4\sigma_s$ is the full bunch length, $h_{rf} = 35640$ the rf harmonic number and V_{rf} the peak rf-voltage

$$L = \begin{cases} 0.52 \text{ m} & \text{at 450 GeV,} \\ 0.30 \text{ m} & \text{at 7 TeV,} \end{cases} \qquad V_{rf} = \begin{cases} 8 \text{ MV} & \text{at 450 GeV,} \\ 16 \text{ MV} & \text{at 7 TeV.} \end{cases}$$

The total effective impedance is the sum of the broad-band and of the low-frequency contributions

$$(Z_L/n)_{eff} = (Z_L/n)_{eff}^{bb} + (Z_L/n)_{eff}^{lf} = j \begin{cases} (0.131 + 0.144)\,\Omega = 0.275\,\Omega & \text{at 450 GeV,} \\ (0.137 + 0.087)\,\Omega = 0.224\,\Omega & \text{at 7 TeV.} \end{cases}$$

Therefore, since $I_b^{th} = N_b^{th} e \omega_0 / 2\pi$, we obtain the following rather high threshold bunch populations

$$N_b^{th} \simeq \begin{cases} 6.4 \times 10^{12} & \text{at 450 GeV,} \\ 3.0 \times 10^{12} & \text{at 7 TeV.} \end{cases}$$

The coherent tune shifts induced by the broad-band impedance for high-order longitudinal modes should remain smaller than the synchrotron tune spread

$$\Delta Q_s = \frac{\pi^2}{16} \left(\frac{h_{rf} L}{2\pi R} \right)^2 Q_s .$$

Using Eq. (1) and assuming a safety factor 4 for the ratio $\Delta Q_s / \Delta Q_L$, we obtain the following threshold bunch current corresponding to suppression of Landau damping

$$I_b^{th} \simeq \frac{3\pi^2}{64} \frac{h_{rf}^3 V_{rf}}{\text{Im}\,(Z_L/n)_{eff}^{bb}} \left(\frac{L}{2\pi R} \right)^5 .$$

The associated maximum bunch populations at injection and at top energy are

$$N_b^{th} \simeq \begin{cases} 2.0 \times 10^{12} & \text{at 450 GeV,} \\ 2.4 \times 10^{11} & \text{at 7 TeV.} \end{cases}$$

Therefore, the most dangerous single-bunch longitudinal effect in the LHC is the possible suppression of Landau damping at 7 TeV; however this would occur only at more than twice the nominal bunch population.

7.2 *Transverse single-bunch effects*

The dominant single-bunch instability in the case of transverse oscillations is the mode-coupling instability, occurring when the relative tune-shift of two adjacent head-tail modes equals the synchrotron tune Q_s. The corresponding threshold current, approximately equal also to that for the transverse microwave instability, is

$$I_b^{th} \simeq \frac{2Q_s E/e}{\beta_{av} \mathrm{Im}\,(Z_T)_{eff}} \frac{L}{R}.$$

The total transverse impedance is the sum of the broad-band and of the low-frequency contributions

$$\beta_{av}\,(Z_T)_{eff} = \beta_{av}\left((Z_T)_{eff}^{bb} + (Z_T)_{eff}^{lf}\right)$$

$$= j \begin{cases} (-62.8 + 628.2)\ \mathrm{M\Omega} = 565.4\ \mathrm{M\Omega} & \text{at 450 GeV,} \\ (351.0 + 366.8)\ \mathrm{M\Omega} = 717.8\ \mathrm{M\Omega} & \text{at 7 TeV.} \end{cases}$$

The associated maximum bunch populations at injection, when $Q_s = 5.4 \times 10^{-3}$, and at top energy, when $Q_s = 1.95 \times 10^{-3}$, are therefore

$$N_b^{th} \simeq \begin{cases} 5.9 \times 10^{11} & \text{at 450 GeV,} \\ 1.5 \times 10^{12} & \text{at 7 TeV.} \end{cases}$$

A more accurate estimate of the mode-coupling threshold at injection can be obtained using the tune shifts of the head-tail modes with $n = 0$ and $|n| = 1$ given in Table 1, 3, 6, 4 and 5 for the coherent space charge, the broad-band resonators, the pumping slots, the strip-line monitors and the abort kickers, respectively,

$$\Delta Q_T = \begin{cases} (7.49 - 5.80 - 0.63 - 7.56 - 3.08) \times 10^{-4} = -9.58 \times 10^{-4} & \text{for } n = 0, \\ (3.75 - 2.92 - 0.31 - 0.05 - 0.13) \times 10^{-4} = 0.34 \times 10^{-4} & \text{for } n = -1. \end{cases}$$

This gives a slightly lower threshold

$$N_b^{th} \simeq \frac{Q_s}{\Delta Q_T^{(-1)} - \Delta Q_T^{(0)}} \times 10^{11} \simeq 5.4 \times 10^{11}.$$

Assuming a nominal bunch population $N_b = 10^{11}$ particles, the transverse tune shift induced at injection by the broad-band impedance for a high-order head-tail mode of order n is

$$\Delta Q_T^{(n)} = -\frac{1}{n+1} \frac{I_b R}{2(E/e)L} \beta_{av} \mathrm{Im}\,(Z_T)_{eff}^{bb} \simeq \frac{1 \times 10^{-4}}{n+1}, \qquad \text{for } n \geq 1.$$

The space charge tune spread $\Delta Q_{sc} \simeq 1.2 \times 10^{-3}$ is therefore sufficient to provide Landau damping of the high-order transverse modes. The tune shift of the transverse dipole mode,

mainly induced by the low-frequency impedance, is $\Delta Q_{\mathrm{T}}^{(0)} \simeq -1 \times 10^{-3}$ and stability can be ensured if a comparable tune spread (*other* than the space charge tune spread) is present in the beam, either due to natural magnetic non-linearities or to the system of octupolar lenses.

8 COUPLED-BUNCH INSTABILITIES DUE TO RF-CAVITY MODES

A detailed analysis of possible coupled-bunch instabilities driven by the narrow-band impedance of superconducting and feedback cavities can be found in Reference 15. The frequency and R/Q of the most prominent high order modes (HOM) have been computed using the code URMEL: these parameters depend only on the geometry of the rf-cavities. For each HOM (assuming all the others to be non-existent) the code BBI is then used to estimate the coherent tune shifts of all the coupled-bunch modes; for HOM's of the superconducting cavities, where the coherent modes of both beams can be coupled by the common impedance, the tune shifts are computed for a single beam with twice the nominal bunch intensity. A comparison of the coherent tune shifts with the synchrotron tune spread (for longitudinal modes) or with the space charge tune spread (for transverse modes) leads to a maximum Q value of that particular HOM compatible with Landau damping. The result is that a moderate damping of most HOM's with Q values in the order of 10^4 is sufficient to ensure beam stability. A few HOM's, especially in the septum cavities, may require further damping with a tuned antenna.

9 TRANSVERSE RESISTIVE WALL INSTABILITY

The transverse resistive wall instability rise time τ can be written

$$\frac{1}{\tau} = \frac{N_{\mathrm{b}} k_{\mathrm{b}} r_{\mathrm{p}} \omega_{\mathrm{o}}^2}{2\pi\gamma c Z_{\mathrm{o}}} \beta_{\mathrm{av}} \mathrm{Re}\,(Z_{\mathrm{T}})\,, \tag{8}$$

where Z_{T} is the transverse impedance at the frequency ω of the lowest unstable coupled-bunch mode. To avoid significant restrictions on the choice of working point, in the case of LHC we make the pessimistic assumption $\omega/2\pi \sim 3.3$ kHz, corresponding to a fractional betatron tune *below* an integer by 0.3. For a round pipe of radius b, consisting of an inner metallic layer of thickness t and resistivity ρ, surrounded by an outer metallic layer of thickness t' and resistivity ρ', we have

$$Z_{\mathrm{T}} = \frac{2c}{\omega} \frac{R\rho}{b^3 \delta} (1 + j)\, \xi.$$

Here $\delta = \sqrt{2\rho/\mu_{\mathrm{o}}\omega}$ is the skin depth and ξ the two-layer penetration factor, given by the following expression[b]

[b] Expression (4.38) used in the SSC Conceptual Design[5] is wrong, since it does not reduce to the correct single-layer formula[4] when $\rho=\rho'$.

$$\xi = \frac{f + \rho_{\rm rel} f'}{1 + \rho_{\rm rel} f f'}, \qquad \rho_{\rm rel} = \sqrt{\frac{\rho'}{\rho}} \qquad f(\delta, t) = \frac{1 - \exp[-2(1+j)t/\delta]}{1 + \exp[-2(1+j)t/\delta]},$$

where ρ, δ and $f(\delta, t)$ refer to the inner layer, while ρ', δ' and $f' = f(\delta', t')$ refer to the outer layer.

Since the instability rise time in a pipe with *square* cross section[16] of side a is the same as for a *round* pipe of diameter $2b = 1.103 \times a$, for the LHC beam screen we can use our formula (8) with an effective radius $b \simeq 0.55 \times 34.8 = 19$ mm. Assuming a large thickness $t_{\rm ss} \sim 10$ mm for the stainless steel beam screen (which, from this point of view, behaves as if it were in contact with the cold bore[11]) and a temperature $T \sim 20°$K, in Table 9 we report the resistive wall instability rise times at injection energy, corresponding to different values of the copper layer thickness $t_{\rm Cu}$ under the hypothesis that all the machine be cold. The skin depths in copper and in stainless steel are $\delta_{\rm Cu} \simeq 0.1$ mm and $\delta_{\rm SS} \simeq 6.2$ mm, respectively.

The effect of highly resistive regions (welds) at the top and bottom of the beam screen is difficult to assess quantitatively since:

1. The azimuthal extent of these regions ($\sim$ 1 mm) is smaller than the corresponding skin depth at 3.3 kHz ($\delta \sim 6$ mm, assuming stainless steel resistivity for the welds): therefore the boundary conditions for field matching should properly take into account the transition regions on both sides of each weld, with an azimuthal extent presumably of order δ,

2. the outer cold bore plays a role, although very little field can be expected to leak out of the welds owing to the previous remark,

3. The lack of isotropy may lead to a tensor transverse impedance.

However, the rise time of the transverse resistive wall instability is dominated by the warm sections of the machine. If 10% of the beam pipe consists of a 2 mm thick copper chamber at room temperature (with $\rho_{\rm Cu}^{\rm warm} = 1.5 \times 10^{-8}$ Ωm, $\delta_{\rm Cu}^{\rm warm} \simeq 1$ mm and the same

TABLE 9: Transverse resistive wall instability rise times at injection, for a beam screen temperature T=20°K and different values of the copper layer thickness $t_{\rm Cu}$.

copper layer thickness $t_{\rm Cu}$ [μm]	penetration factor ξ	weighted impedance $\beta_{\rm av}{\rm Re}(Z_{\rm T})$ [GΩ]	instability rise time τ [msec]
50	$1.3-j\,1.0$	5.4	28
40	$1.6-j\,1.3$	6.7	23
30	$2.0-j\,1.7$	8.8	17
20	$3.0-j\,2.6$	13.0	12
10	$5.8-j\,4.8$	24.6	6

geometry and average beta as in the remaining cold pipe), for a 50 μm copper coating of the beam screen at 20°K the instability rise time is reduced from 28 to 21 msec. For a screen temperature of 50°K, the corresponding rise time would be 9 msec, i.e., shorter than 100 revolution periods. An upper bound for the effect of the welds is therefore sufficient at this stage of the LHC design and, according to numerical estimates based on discontinuous Leontovich boundary conditions at the transitions between copper layer and welds,[17] the instability rise time is reduced by no more than 20% if the azimuthal extent of each weld is below 2.5 mm.

10 PARASITIC LOSSES

The design of the LHC beam screen results from an optimization of its geometrical, mechanical, thermal and electromagnetic properties.[18] In particular, the thickness of the inner copper layer is constrained to small values to minimise eddy current forces in case of a magnet quench and to large values to reduce the low-frequency resistive wall impedance, responsible for transverse coupled-bunch instabilities. An original proposal to have only four copper strips, instead of a uniform copper coating, would have solved the problem of quench forces; however the ohmic losses due to image currents induced by the beam in the uncoated high-resistivity regions (about 50% of the screen surface) would have been unacceptable.[11] Indeed, the resistive losses in stainless steel are about $\sqrt{\rho_{ss}/\rho_{Cu}} \simeq 30$ times larger than in copper at cryogenic temperatures (assuming $\rho_{Cu} = 5.5 \times 10^{-10}\,\Omega$m) and, over most of the bunch spectrum, image currents can be computed just by solving the electrostatic two-dimensional problem with boundary conditions independent of the wall resistivity.

In case of uniform copper coating, the resistive wall losses for a square liner of side a are the same as the losses in a circular liner of radius $b = a/2$. A numerical solution of the electrostatic problem shows that these losses are also the same for the LHC square liner with rounded corners, having radius of curvature equal to $a/4$. Therefore, using the formula for a circular liner of radius $b = 17.4$ mm, the power loss is given by

$$P_w = \Gamma\left(\frac{3}{4}\right)\frac{k_b}{b}\left(\frac{N_b e c}{2\pi}\right)^2\sqrt{\frac{\rho_{Cu}Z_o}{2}}\sigma_s^{-3/2} \simeq \begin{cases} 0.45\ \text{kW} & \text{at 450 GeV,} \\ 1.97\ \text{kW} & \text{at 7 TeV,} \end{cases}$$

where we have assumed a screen temperature of 20°K and a nominal bunch population $N_b = 10^{11}$ particles. This result does not change appreciably if the anomalous skin-effect is taken into account.[11]

The numerical solution of the electrostatic problem also shows that the ratio between the image current density induced at the centre of the rounded corners and that for a circular inscribed liner is almost exactly $1/2$. Therefore a high-resistivity region of small azimuthal extent $\Delta\ell \ll b$ (e.g., a weld with resistivity ρ_{ss}), located at one of the rounded corners increases the ohmic losses by

$$\frac{\Delta P_w}{P_w} \simeq \frac{1}{4}\sqrt{\frac{\rho_{SS}}{\rho_{Cu}}}\frac{\Delta\ell}{2\pi b}.$$

For two welds at the top and bottom of the LHC screen, each having a width $\Delta\ell = 1$ mm, the corresponding resistive wall losses are increased by 14%.

To obtain an upper bound for the power loss through the pumping slots, we consider circular holes of diameter equal to the slot width $2r_h = w = 1.5$ mm, covering the same fractional surface $f = 4.3\%$ of a circular screen with radius $b = 17.4$ mm. Therefore, we neglect the geometric reduction factor of 0.79 for the induced image current at the slot position and the further reduction of power loss through slots compared to that through circular holes, confirmed by recent measurements by F. Caspers. However, even for an infinitely thick wall, $H_{0,1}$ waves with cut-off frequency $\pi c/\ell$ can propagate through a slot of length ℓ. The issue of how efficiently these waves can be excited by the beam and the consequent tolerances on the slot alignment with respect to the beam axis remain to be clarified. The power loss through circular holes of radius r_h, covering a fractional surface f in a circular screen of radius b, thickness t, outer resistivity ρ, surrounded by an outer circular pipe of radius b' and resistivity ρ', is given by[19]

$$P_h = \Gamma\left(\frac{5}{4}\right) k_b \left[\frac{N_b e}{3\pi^2} f r_h F\left(\frac{t}{r_h}\right)\right]^2 \frac{Z_o\sqrt{2\mu_o/\rho}}{\sigma_\tau^{5/2} b\left(1+\frac{b}{b'}\sqrt{\frac{\rho}{\rho'}}\right)},$$

where the function $F(t/r_h)$ is associated with attenuation from the 'inside' to the 'outside' of the hole through the circular wave guide of radius r_h and length t equal to the hole depth:

$$F(x) = 2e^{-1.841x}\left[1 - 0.19\left(1 - e^{-3.682x}\right)\right] - e^{-2.405x}\left[1 - 0.14\left(1 - e^{-4.81x}\right)\right].$$

Assuming the same resistivity $\rho = \rho' = \rho_{ss} = 5 \times 10^{-7}\ \Omega$m for the outer surface of the beam screen and of the cold bore, for a screen thickness $t = 1$ mm and a cold bore radius $b' = 24.15$ mm, the power loss through circular holes is 0.26 kW. To help reducing the fraction of this power dissipated at the cold bore, it is foreseen to arrange microwave absorbers attached to the outside surface of the LHC screen (not touching the 2°K surface of the cold bore). Since the attenuation length of the coaxial region between beam screen and cold bore would then become shorter, these microwave absorbers can also significantly reduce the coherent build-up of the TEM waves travelling in synchronism with the beam and thus the corresponding power loss through the pumping slots.

The parasitic losses for LHC at top energy are summarized in Table 10. We have included an upper bound for the power loss due to coherent synchrotron radiation (possibly largely overestimated) and for the leakage of electromagnetic energy through a gap $\Delta = 0.01$ mm between the sliding contacts of the bellows.[7] The latter is certainly a rather pessimistic assumption, in view of the new bellows design including spring fingers at the entrance of the gap. The parasitic losses in the shielded bellows have been estimated using the broad-band resonator parameters of Table 2. However, as in the case of the monitor tanks, the broad-band resonators are not meant to model the real part of the longitudinal impedance; the corresponding losses represent therefore only an upper bound.

TABLE 10: Summary of parasitic losses for LHC at 7 TeV.

Power loss [kW]	For a Single Beam	Power loss per unit length [mW/m]
3.67	Incoherent synchrotron radiation	216
$\ll$0.54	Coherent synchrotron radiation	$\ll$32
1.97	Resistive wall (20°K)	74
0.27	Welds	10
0.26	Pumping slots	10
<0.80	Shielded bellows	<30
$\ll$1.03	Leaks in bellows gaps	$\ll$38
8.54	Total	410

11 CONCLUSIONS

Instability thresholds and parasitic losses have been estimated using somewhat conservative assumptions. However the LHC impedance budget is not complete and more detailed calculations are still required, although we believe that the most significant contributions have been taken into account. The possibility of a transient bunch-to-bunch detuning during injection and the consequences of closed orbit residuals on the betatron coupling are important topics for future studies: together with a more careful computation of the magnetic Laslett tune shift, they have implications on the injection tolerances and on the strategies for orbit correction and coupling compensation.

Further experimental and theoretical investigations on trapped and high-frequency modes caused by the pumping slots in the beam screen are in order. Their electromagnetic properties, such as detuning due to slot randomization or damping associated with mode conversion at the slots,[20] can be measured and their effects on the beam dynamics should be computed.

Power losses through the pumping slots associated, e.g., with a possible microwave structure of the beam spectrum, should also be investigated. This may have an impact on the final design of the beam screen, including the optimal choice of the slot length and the arrangement of microwave absorbers in the outer coaxial region between the screen and the cold bore.

REFERENCES

1. F. Sacherer, *IEEE Tran. Nucl. Sci.*, **NS-24**, 1393 (1977) and CERN Report 77–13, p. 198 (1977).
2. S. Petracca, CERN Report SL/93–13 (AP), 1993 and *Part. Acc.*, **48**, 181 (1995).
3. L.J. Laslett, in *Proc. of the 1963 Summer Study on Storage Rings, Accelerators and Experimentation at Super-High Energies*, Brookhaven, ed. J.W. Bittner, BNL Report 7534, p. 324 (1963).

4. A.W. Chao, *Physics of Collective Beam Instabilities in High Energy Accelerators*, (Wiley, New York, 1993).
5. K.Y. Ng, Fermilab Report FN-443 (1987) and *SSC Conceptual Design*, SSC Report SR-2020, ed. J.D. Jackson (1986).
6. L. Vos, CERN LHC Note 47 (1987).
7. The LHC Study Group, *Design Study of the Large Hadron Collider (LHC)*, CERN Report 91–03 (1991).
8. L. Vos, private communication (February 1995).
9. G. Shröder, communications, this workshop.
10. S.S. Kurennoy, in *Proc. of the IEEE 1993 Particle Accelerator Conference*, Washington, D.C., p. 3420 (1993) and B. Zotter, *Part. Acc.*, **1**, 311 (1970).
11. M.M. Karliner, N.V. Mityanina, B.Z. Persov and V.P. Yakovlev, proceedings to this workshop.
12. A. Chao, proceedings to this workshop.
13. S.S. Kurennoy, proceedings to this workshop.
14. J. Gareyte, private communication (November 1994).
15. D. Boussard and E. Onillon, CERN SL Note/93–116 (RFS), 1993.
16. M.M. Karliner, N.V. Mityanina, B.Z. Persov and V.P. Yakovlev, *LHC beam screen design report* (Preprint BudkerINP 94–45, Novosibirsk, 1994).
17. V.P. Yakovlev, communications, this workshop.
18. B. Angerth, F. Bertinelly, J.-C. Brunet, R. Calder, F. Caspers, O. Gröbner, A.-G. Mathewson, A. Poncet, C. Reymermier, F. Ruggiero and R. Valbuena, *The LHC beam screen–specification and design*, presented at the 1994 EPAC Conference, London.
19. F. Caspers, E. Jensen and F. Ruggiero, in *Proc. of the EPAC Conference*, Berlin, p. 889 (1992), (Editions Frontières, Singapore, 1992).
20. F. Caspers, private communication (January 1995).